

PHOTOMETRIC REDSHIFT TECHNIQUES: ¹ RELIABILITY AND APPLICATIONS

H. K. C. Yee

Department of Astronomy, University of Toronto, Toronto, M5S 3H8, Canada.

Abstract

The idea of using multi-band photometry to estimate the redshifts of galaxies has a long history, but it is only recently that it has come to widespread use and acceptance. This paper describes the recent developments and applications of photometric redshift techniques. There are two major approaches to photometric redshift techniques: spectral energy distribution (SED) fitting, using either observed SEDs or population synthesis model SEDs; and empirical methods using spectroscopic samples as training sets. The availability of Hubble Deep Field data in four bands has provided a great impetus in using photometric redshifts. A detailed discussion of the robustness of the results is presented. The usefulness of redshift information derived from photometric data with limited number of filters (as few as two) is also discussed. Taking all current evidence together, it appears that photometric redshift can be a reliable and extremely useful technique with many applications, if care is taken to ensure that systematic effects and catastrophic redshift errors are minimized.

1 Introduction

The idea of using broad-band photometry to estimate the redshifts of galaxies was suggested as early as 35 years ago by Baum (1963). The basic concept is simple: multi-band photometry can be regarded as a very low resolution spectrum, and hence can be used to estimate the redshifts of galaxies and other extragalactic objects. Although this idea has been applied by a number of investigators in the ensuing years, it was only in the past few years that photometric redshifts have found widespread application and acceptance.

With the availability of deep, wide-field CCD photometry today, the potential scientific return of photometric redshifts is great. There are essentially two major applications of the method. The first is to provide redshift samples in a quick and inexpensive way. Although the typical redshift uncertainty is expected to be in the range of 0.05 to 0.10, far less accurate than that expected from a spectroscopic survey, many scientific goals can still be attained with a photometric redshift sample; for examples: the determination of luminosity functions (e.g., SubbaRao et al. 1996; Mobasher et al. 1996, Gwyn & Hartwick 1996; Sawicki, Lin, & Yee 1997, hereafter SLY97), luminosity densities (e.g., SLY97; Connolly et al. 1997; Madau et al.

¹To appear in the proceedings of the Xth Rencontres de Blois: *The Birth of Galaxies*

1998); and the projected spatial correlation function (e.g., Connolly, Szalay, & Brunner 1998; Miralles & Pelló 1998). The second major application is to provide estimates of the redshifts of objects which are too faint for conventional spectroscopy.

In this review, I will begin with some historical notes on the method of photometric redshifts, describe the recent developments, and comment on the reliability and recent applications of the method. The technique of using simply two or three color bands for selecting a sample of objects at a certain redshift, which is the photometric redshift method in its crudest form, will also be discussed.

2 Photometric Redshift Techniques

2.1 Some Historical Notes

The first systematic application of photometric redshift was carried out by Baum (1963) who obtained photoelectric photometry of early-type galaxies in distant galaxy clusters using 9 bands. He estimated the redshifts of the clusters by comparing the spectral energy distributions (SEDs) with those from galaxies in the Virgo Cluster, using primarily the position of the 4000Å break in early-type galaxies.

Koo (1985) analysed the dependence of 4-band data from photographic photometry on redshift. By making linear combinations of the 4 filters, he was able to show that one can form “iso- z ” loci on color-color plots, and hence provide a “poor-person’s redshift machine”.

A strong effort in applying photometric redshifts to a specific astronomical problem was first made by Loh & Spillar (1986). They used CCD photometry in 6 filters and obtained redshifts by fitting galaxy SEDs of various morphological types, and attempted to determine Ω via galaxy number density as a function of redshift.

Many of the early efforts, however, were hampered by the lack of high quality, wide-field digital data, and the difficulties of obtaining a significant and convincing set of verification redshifts.

2.2 Modern Developments

After these early efforts, there was a hiatus of almost 10 years before photometric redshifts came into vogue again. There are several reasons why photometric redshifts have enjoyed such a rigorous revival. One is the advent of better and, more importantly, much bigger CCD detectors. The larger field size, culminating in the mosaic CCDs with field sizes up to a square degree that are now being built at most modern observatories, makes obtaining deep multi-color photometry of a large sample of galaxies in an efficient manner possible. Another recent major thrust for the photometric redshift technique is the availability of the Hubble Deep Field (HDF, Williams et al., 1996) which contains multi-color data of galaxies to the depth of 29 mag, much too faint for conventional spectroscopy.

The modern photometric redshift techniques can be divided into two major approaches. One is the more traditional method of fitting model galaxy SEDs to the photometric data; the other is the newer technique of using a spectroscopic redshift sample as training set for the photometric redshift sample.

It should be noted that regardless of which technique is used, the efficacy of the method depends on the spectral type of the galaxy and the wavelength region covered by the observed wave bands. The primary redshift signal from photometric data arises from prominent breaks in the galaxy SED, such as the 4000Å/Balmer breaks, and the Lyman break. The slope of

the photometric measurements on either side of the break produces additional refinements in the redshift estimate. The overall continuum curvature of the SED, along with the break size, provides information on the spectral type. Hence, it is expected that galaxies with large spectral breaks which are straddled by the filter bands (preferably with at least one band completely on each side of the break) will have the most robust and accurate measurements. For example, for data solely in the observed optical bands, early-type galaxies at low redshift ($z < 0.8$, beyond which the 4000Å break enters the I band), or star-bursting galaxies at high redshift ($z > 3$, where the Lyman break enters the U band) will have the strongest redshift signal. On the other hand, low-redshift star-forming galaxies or any galaxies at z between 1 and 3 will have more uncertain redshift signatures.

2.2.1 *The SED Fitting Method*

All of the early work on photometric redshifts (Baum 1963; Koo 1985; and Loh & Spillar 1986) essentially used the SED template fitting method, with Loh & Spillar being the first to explicitly fit SEDs of various types of galaxies to the data by minimizing χ^2 . The SED fitting technique is necessary if there is no training set of redshift data to derive empirically the relationship between colors and redshift. Although the method has a certain simplicity in the way it is applied, a major uncertainty arises from not knowing the precise template set to be used. In general, two approaches have been taken. The first is to use empirical spectro-photometric SEDs obtained from relatively low redshift galaxies, with the most often used templates being the SEDs of different spectral types in Coleman, Wu & Weedman (1990, hereafter CWW). An alternative is to use theoretical SEDs from population synthesis models, such as, for example, the GISSEL models of Bruzual & Charlot (1993, 1996).

A great impetus for using this technique was provided by the HDF data, as the great depth of these photometric data excludes the possibility of obtaining a fair spectroscopic redshift sample fainter than ~ 24 mag as the training set. At high redshift, complications arise due to the lack of suitable high quality empirical SED data at short wavelengths, as the UV spectrum is shifted into the optical band. Furthermore, high redshift galaxies may have significantly different SEDs from those of local galaxies even if we are able to obtain good UV SEDs of local galaxies. This has led to the use of hybrid templates combining local empirical SEDs with model SEDs at the short wavelength regime (e.g., see SLY97). A further complication is the attenuation of the UV spectrum arising from intergalactic hydrogen. Although most practitioners statistically correct for this absorption (mostly using the method of Madau 1995), the actual amount of absorption in any line of sight is stochastic, introducing additional uncertainties.

A large number of groups (for a partial list, see Hogg et al. 1998) have derived photometric redshifts for galaxies in the HDF to as faint as 27 to 28 mag with redshifts running as high as $z = 6$. The fitting methods used include minimizing χ^2 (e.g., SLY97; Gywn & Hartwick 1996) and maximizing likelihood functions (e.g., Lanzetta, Yahil, and Fernandez-Soto 1996). These results serve as an excellent illustration of the dependence of the results on the choice of SED templates, and a more detailed discussion is given in Section 3.2.

2.2.2 *The Empirical Training Set Method*

The empirical photometric redshift technique requires a training set of data in which both the redshifts and photometry are available. The method tries to obtain an optimal fit between the photometric and redshift measurements, and uses this fit to predict the redshift of objects with only photometric data. Although this method has the advantage of being empirical, and hence is not dependent on having exact knowledge of the SEDs of galaxies, obtaining a proper and sufficiently large training set is very often expensive observationally. Furthermore,

extrapolating the fit to galaxies with magnitudes or redshifts outside the ranges of the template set must be done with great care, as it will produce additional unknown uncertainties.

The most detailed application of such a technique has been carried out by Connolly et al. (1995). They used a sample of 254 galaxies with redshifts and 4-band (basically *UBRI*) photographic photometry with a magnitude limit of $B_J \leq 22.5$. The correlation between photometry and redshift was analysed in the multi-dimensional space of the flux measurements. They reported that a simple linear regression fit of z as a function of the magnitudes from the 4 filters produced a rms dispersion, σ_z , of 0.057. A quadratic fit, which requires a total of 17 terms in the 4 filters, reduced σ_z to 0.047. They also showed via simulated data that fitting data that are binned into redshift bands by an iterative procedure can reduce the dispersion to less than 0.02. They found that additional bandpasses do not add more accuracy. However, this is most likely due to the fact that the method has been applied to a relatively narrow range of redshift (0.0 to 0.6). This group has further verified the accuracy of their method using a much smaller number of objects with CCD photometry (Brunner et al. 1997).

Wang et al. (1998) used a modified version of the Connolly et al. method to derive photometric redshifts from the HDF. Their method fits the spectroscopic redshift to a linear function in the 3 dimensional color space, instead of the 4 dimensional flux space.

A very different approach, combining SED fitting and the empirical training methods, is being taken by the CNOC (Canadian Network for Observational Cosmology) group (Sawicki et al., 1999), and we present a preliminary report on this ongoing work. The CNOC2 field redshift survey (Yee et al. 1998, 1999) contains over 5000 redshifts of galaxies to $R_c \leq 21.5$ mag with $z < 0.75$; the current results are based on about 1/4 of the sample. Because of the large sample size and the availability of five-color CCD photometry (*UBVRI*) for almost all objects, the CNOC2 survey is an ideal sample for applying and testing the empirical photometric redshift technique. We use a “hybrid” technique which first finds the best fitting SED templates for the training set, and then trains the template set by adjusting the templates as a function of SED types and *redshift* to fit the data optimally. This trained template set can then be used to obtain redshifts from other photometric data. We note parenthetically that there is a major conceptual difference between the CNOC method and that of the Connolly et al. method: the CNOC method does not depend on the apparent magnitude of the galaxy for any of the redshift signal. Using the flux as part of the redshift signal may produce subtle biases in an apparent magnitude limited sample, a conjecture which we will be able to check using the large CNOC2 database.

Using this method we are able to obtain preliminary results with σ_z of ~ 0.06 for objects with a signal-to-noise (S/N) ratio better than 10. Figure 1 plots Δz between spectroscopic and photometric redshifts as a function of R_c magnitude and redshift for 1387 objects. The sample can also be divided up into different spectral types (via the 5-color photometry). The results show a worsening of σ_z with later-type spectra (as expected), but no systematics in Δz with either magnitude or redshift.

3 Reliability of Photometric Redshifts

3.1 Redshift Uncertainty

The empirical methods of Connolly et al. (1995) and Sawicki et al. (1999) show that with 4 or more filters and a S/N ratio of ~ 10 , an accuracy of $\sigma_z \sim 0.05$ can be achieved over the redshift range of 0 to 0.8. In the case of the CNOC2 data set (Sawicki et al. 1999), the sample is large enough that one can actually use a subsample to train the templates, and then test

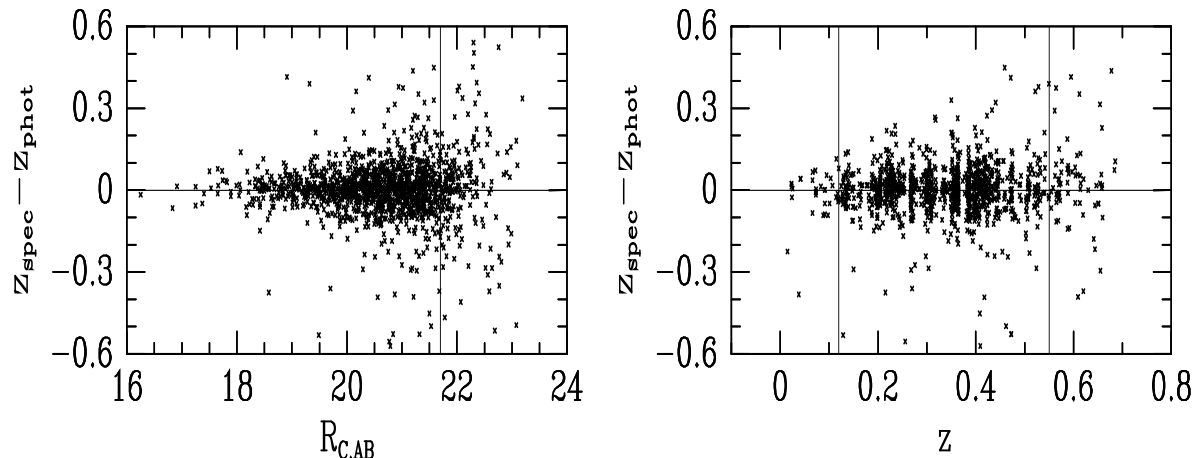


Figure 1: Δz vs R magnitude and z for 1387 galaxies in the CNOC2 Field Galaxy Survey sample used as training set. The vertical lines indicate the nominal spectroscopic limit in $R_{C,AB}$ and the fair sample redshift range. The rms of Δz is about 0.07 for the whole sample. Note the lack of systematic trend with either magnitude or z .

the templates on the remaining large set of galaxies with known redshifts. Similarly, various authors have shown that comparing their photometric redshifts from the HDF obtained by SED fitting with available spectroscopic redshifts indicates typical agreements of $\Delta z \sim 0.1$. (A detailed discussion of the robustness of the HDF photometric redshifts will be given in Section 3.2.)

Although direct statistical comparisons of photometric and spectroscopic redshifts appear to produce satisfactory results, there is another important type of redshift errors that must be assessed. This is termed by Yee, Ellingson, & Carlberg (1996) as “catastrophic errors” in their discussion of errors in spectroscopic redshift surveys. This type of errors could arise from the misidentification of either emission or absorption line features, or in the the case of using cross-correlation techniques, of the cross-correlation peak. The same problem exists for photometric redshift techniques. A catastrophic error in photometric redshift determination occurs when two templates with very different redshifts occupy regions in the multi-color space that are too close together, so that for a variety of reasons, the template with the incorrect redshift is chosen. This could be the result of poor signal-to-noise ratio in the data, unrealistic templates being used, or simply a real degeneracy arising from the very coarse spectral information available within both the data and the templates. (For a detailed description of these effects, see SLY97.) The simplest example of catastrophic error in a sample spanning a sufficiently large redshift range (as is the case for the HDF data set) arises from the confusion of the Lyman break with the 4000\AA break. It is instructive to peruse the redshift likelihood functions plotted in Lanzetta et al. (1996) in which one very often sees two redshift peaks, corresponding to the signals from the two strongest breaks in most galaxy spectra. Picking the correct redshift has the same connotation as picking the correct cross-correlation peak in a spectroscopic redshift analysis.

Catastrophic errors are difficult to assess and catch, and, as we will show in the next Section, can have severe effects on the scientific analysis of the data. A possible way to alleviate this problem is to obtain a larger wavelength coverage; for example, extending into the near-IR bands. The larger coverage will either provide significantly more information on the continuum curvature on both side of a break, or, in some cases, sample more than one break simultaneously, considerably reducing the ambiguity. We note that Fernandez-Soto et al. (1998) and Connolly

et al. (1997) supplemented the optical HDF data with ground-based IR data to improve their redshift determination.

3.2 The Hubble Deep Field as a Case Study

The publicly available HDF data instigated a major revival of interest in photometric redshifts. The very deep images in 4 bands provide an excellent data set for applying the technique to unprecedented depth and redshift, allowing us to study galaxy evolution over 90% of the age of the Universe. At this point, very few scientific applications of redshift catalogs from photometric redshift samples have been published other than those based on the HDF.

Several groups created photometric redshift catalogs within half a year of the release of the data (Gwyn & Hartwick 1996, Mobasher et al. 1996, Lanzetta et al. 1996, and SLY97), and more followed in the subsequent year (e.g., Connolly et al. 1997, Miralles & Pelló 1998; Wang et al. 1998). This is the only data set which has been analysed independently for photometric redshifts by a large number of groups, offering us the opportunity to compare results and obtain some idea on the robustness of photometric redshift determinations.

Here, we can make two kinds of comparisons. One is the accuracy of the redshift determination as compared with the increasingly large sample of objects in the HDF with spectroscopically measured redshifts (most, if not all, from the Keck Telescope). This comparison would apply only to the set of objects that have been spectroscopically measured. Most of the investigations mentioned above have plotted photometric- z versus spectroscopic- z in their paper, and most showed excellent agreements, with typical spread of $\Delta z \sim 0.1$, and also a small number of catastrophic redshift errors. Hogg et al. (1998) specifically conducted a blind test of photometric redshifts versus a small magnitude-limited spectroscopic redshift sample with objects having mostly $z < 1.5$. Five different groups participated in the test, and again, the results showed that $\Delta z \sim 0.1$ were obtained by all groups.

It should be noted, however, that this basic agreement (disregarding the catastrophic errors, which, as it turned out, could also be due to erroneous redshift determinations in the spectroscopic sample; see Lanzetta et al. 1997b, and Sawicki & Yee 1998) applies only to the spectroscopic sample, which may not be a homogeneous or fair magnitude-selected sample. First, the spectroscopic sample is based on galaxies that are mostly < 24.5 mag, whereas the photometric samples extend the magnitude range considerably, to as faint as 28 mag. Second, the $z > 2$ spectroscopic sample is almost exclusively comprised of objects preselected to be Lyman-break galaxies based on colors, which are also galaxies with the largest photometric redshift signals at these redshifts. The population of fainter, possibly non-star bursting, $z > 2$ galaxies are not represented in these direct comparisons. Furthermore, there is a dearth of spectroscopic redshifts in the redshift range of $1 < z < 2$, simply due to the difficulties in measuring redshifts in this range with an optical spectrograph. Hence, the apparent agreements between photometric and spectroscopic redshifts may be over-stated.

An equally important comparison is that between the photometric redshifts for all the objects obtained by the different groups. In the case for the HDF data where SED fitting is the dominant technique used, the primary cause for different results amongst the various groups is in the details of the template sets used. Here, we examine the effects of the template sets, and their consequence on the interpretation.

Of the published photometric redshift works on the HDF from which we can make direct comparisons of the redshift distributions or derived luminosity functions, there are basically two variations of template sets: population synthesis models (e.g., Gwyn & Hartwick 1996; Mobasher et al. 1996; and Miralles & Pelló 1998) and observed SEDs with UV extensions based on synthetic SEDs (e.g., SLY97, and Lanzetta et al. 1996). The other major difference amongst

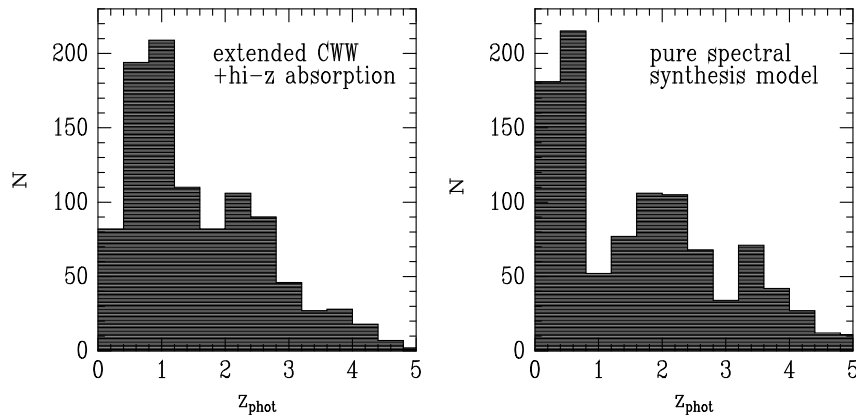


Figure 2: Comparison of photometric redshift distributions of galaxies brighter than $F814W = 27$ mag from the HDF. The left panel shows the distribution obtained by using CWW SEDs extended with GISSSEL models with intergalactic absorption, the right panel shows the distribution obtained by using pure GISSSEL models which are less realistic.

the various groups is that SLY97 and Lanzetta et al. included corrections for intergalactic UV absorption, while the other 3 did not. (However, we note that the Gwyn and Mobasher groups have since modified their methods, see Hogg et al. 1998.)

The different template sets produce significantly different redshift distributions. Gwyn & Hartwick, Mobasher et al., and Miralles & Pelló produced similar redshift distributions which have two peaks: one at $z \sim 0.5$ and another more prominent peak at $z \sim 2$; while SLY97 and Lanzetta et al. derived distributions with a redshift peak near $z \sim 0.8$, and a slow decline out to $z \sim 4$. SLY97 was able to reproduce the double-peak distribution by using simply a pure GISSSEL template set. This is shown in Figure 2. Hence, it is clear that the precise manner in which the templates are chosen can have a profound effect on the redshift distribution. This difference arises from a large number of catastrophic redshift errors, most likely in the pure GISSSEL model results. SLY97 plotted the comparison of photometric redshifts obtained using the extended CWW templates plus Lyman absorption and pure GISSSEL models, showing that catastrophic discrepancies (of up to $\Delta z \sim 1$) primarily occur at $z > 0.8$, where the 4000\AA break would be in the reddest filter (8140\AA) without an anchoring filter further to the red. A confusion between the 4000\AA break and the much weaker break at $\sim 2600 - 2800\text{\AA}$ would produce this aliasing of Δz of about 1. Comparing the redshift catalogs from SLY97, Gwyn & Hartwick (1996), and Lanzetta et al. (1996) directly shows discrepancies of similar magnitudes for objects with $z > 1$ (Sawicki, private communication). We note that the redshift distribution of Wang et al. (1998), derived using an empirical fitting of colors, is in basic agreement with those of SLY97 except for the redshift range between 1 to 2, where there are the greatest number of catastrophic discrepancies. Hence, one can conclude that in specific redshift intervals, where there is confusing, or little or no redshift information in the observed wave bands, redshift determination may contain large (and likely systematic) uncertainties and the results may depend sensitively on the templates used.

The different redshift distributions can produce very different interpretations of the star formation history of the Universe. This is most clearly seen in the luminosity function (LF) of galaxies at high redshift derived by the three groups who have performed the analysis. Gwyn & Hartwick (1996) and Mobasher et al. (1996) produced similar LFs at $z > 2$ with are considerably flatter at both the bright and faint ends with significant excess density over those

of SLY97. As a consequence, the amount of luminosity evolution estimated by the two groups differs from that of SLY97 by a factor of several.

4 Other Applications

4.1 The Roles of Photometric Redshifts in a Spectroscopic Redshift Survey

The redshift information contained in multi-color data can be extremely useful in a spectroscopic redshift survey. For surveys which target objects of specific interest or redshift range, (e.g., members of a galaxy cluster), this information can be used to preselect galaxies for spectroscopic observation. The most spectacularly successful example of this is the systematic survey of $z > 3$ Lyman-break galaxies by Steidel and his collaborators (e.g., Steidel et al. 1996) using U -band drop-outs. In their survey, images in 3 bands are used to select objects which are detected in the two redder bands, but extremely faint in the bluest band. The drop out in the U band is due to the Lyman-break at a redshift of greater than ~ 3 . The sky density of these galaxies is typically 10^3 per square degree at $R \sim 25$, or about 1% of all the objects. Hence, a preselection of targets based on colors makes such a survey possible.

Another useful function of photometric redshift information is in verifying and improving the redshift determination in a general redshift survey. As mentioned above, spectroscopic redshifts suffer from catastrophic errors when a misidentification of features or the correlation peak occurs. Photometric redshift information, either in the form of photometric redshift or simple colors, can be used to verify the redshift. In a large redshift survey, color information can be used for this purpose in the data reduction pipeline, flagging possible redshift errors that may require human intervention. We note that several HDF redshifts have been found to be in error based on discrepancies with the photometric redshifts (see Lanzetta et al. 1997b and Sawicki & Yee 1998). A second application of photometric redshifts in a general redshift survey is using them to assist in recovering spectroscopic redshifts from marginal S/N ratio spectra. In a low S/N ratio spectrum, the true correlation peak often has to compete with other noise spikes due to beating or confusion between real features and features produced by noise or bad sky subtraction. The photometric redshift can be used to narrow down the possible redshift range of the object, allowing the search for a significant correlation peak over a smaller redshift space. In the CNOC2 redshift survey with its extensive 5-color database, the photometric redshift information is used both to verify measured redshifts and to extend the redshift catalog (Yee et al. 1999)

4.2 The Red Sequence in Galaxy Clusters as a Redshift Indicator

In general, photometric data containing only 2 bands (i.e., one color) are of limited use in extracting redshift information. This is due to the degeneracy in the dependence of a single color on redshift and spectral type. However, in special cases where the morphological type of galaxies are specified, e.g., in the core of galaxy clusters where almost all galaxies are expected to have an early-type spectrum, a single color can provide an extremely accurate estimate of the redshift.

The early-type galaxies in clusters form a color-magnitude relation (CMR) on the color-magnitude diagram with brighter galaxies being redder. These galaxies are also the reddest objects in the cluster – hence the name “red sequence”. From the photometric data of a sample of 45 Abell clusters with redshift between 0.04 and 0.18, López-Cruz (1997) shows that the $B - R$ colors of the red sequence at a fixed apparent R magnitude can be fitted by a quadratic

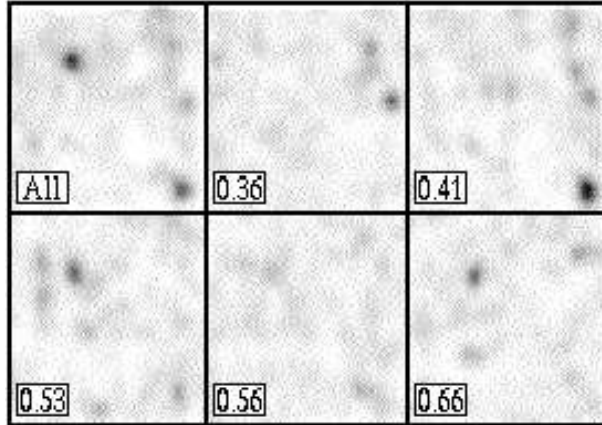


Figure 3: Gray scale plots of galaxy surface density in a $\sim 27 \times 24$ arcmin field from the CNOC2 survey. The “All” panel shows the density of all the data in R band. The other panels show the density in selected CMR color slices with the corresponding redshift shown on the lower left corner. Note the increase in the significance of the peaks in the redshift slice map, and the breaking up of the most prominent peak into two peaks in redshift space.

function to z with a rms dispersion of less 0.008 in z , considerably better than any photometric redshift methods tested so far. The above example is equivalent to the method of using a known redshift sample as a training set. In the case where such a training set does not exist, spectral synthesis models of the CMR, such as those by Kodama & Arimoto (1997), can be used.

Gladders & Yee (1999) have explored using the red sequence method as an inexpensive way of finding clusters/groups from two-band imaging data. The algorithm produces the surface density of galaxies on the sky using galaxies in slices of model CMR in the color-magnitude plane. The color slices correspond to redshift slices, based on models from Kodama & Arimoto (1997). Figure 3 illustrates the result using CNOC2 data as gray scales of galaxy surface density at selected redshift. A number of density peaks are apparent. There are two points of note. First, the significance of the density peaks in general increases when viewed in its redshift slice. Second, one of the peaks in the overall density map breaks up into two peaks at the same position but different redshifts; hence, the redshift slicing by the CMR colors is a very effective in alleviating the problem of line-of-sight projection in searches for groups and clusters. These results have been verified by the spectroscopic redshift data. We also note that these peaks correspond to concentrations that are considerably poorer than Abell Richness Class 0 clusters, making this a very promising one method for finding galaxy groups and clusters.

5 Summary

Photometric redshifts have undergone a great revival of interest in the past few years. This is in part due to the developments in new detectors and new techniques, and in part due to the availability of the very deep HDF data. Both major approaches to photometric redshifts – the use of SED fitting or empirical training sets – have seen considerable advances, and the methods have been applied to very large galaxy samples (e.g., the CNOC2 survey), and galaxies out to large redshifts (e.g., the HDF). Current evidence suggests that typical *statistical* accuracy of Δz of 0.05 to 0.10 can be expected. However, this conclusion is strictly valid only over redshift intervals in which the photometric data contain significant and unambiguous redshift signals. There are two situations which may result in “catastrophic” redshift errors, and hence must

be dealt with great care. These are: confusion of spectral breaks which provide most of the redshift signals and the lack of strong features in the SED within the wavelength range of the data. It is interesting to note these are the very same problems encountered in spectroscopic redshift determinations. Photometric redshift information is also contained in data with two or three filters. These can be used to estimate redshifts of objects with specific properties, such as Lyman-break galaxies and red galaxies in clusters. Photometric redshifts can also be used to verify and improve spectroscopic redshift determination.

In summary, the technique of photometric redshift is an excellent tool with many important applications. However, the accuracy and robustness of the method depend on many factors, and great care must be taken to ensure that systematic effects and catastrophic redshift errors are minimized and understood.

I would like to thank Marcin Sawicki and Mike Gladders for providing the graphics for the paper and insightful discussions, and also Erica Ellingson for useful comments.

References

- [1] Baum, W. 1963, *IAU Sym. 15: Problems of Extragalactic Research*, (New York:Macmillan), p. 390
- [2] Brunner, R.J., Connolly, A.J., Szalay, A.S., & Bershadsky, M.A. 1997, *ApJ*, 482, L21
- [3] Bruzual, A.G. & Charlot, S. 1993, *ApJ*, 405, 538
- [4] Coleman, G.D., Wu, C.C., & Weedman, D.W. 1980, *ApJS*, 43, 393 (CWW)
- [5] Connolly, A., Csabai, I., Szalay, A., Koo, D., Kron, R., & Munn, J. 1996, *AJ*, 110, 2655
- [6] Connolly, A., Szalay, A., Dickinson, M., SubbaRao, M., & Brunner, R. 1997, *ApJ*, 486, L11
- [7] Connolly, A., Szalay, A., & Brunner, R. 1998, *ApJ*, 499, L125
- [8] Gladders, M. & Yee, H.K.C. 1999, in preparation.
- [9] Gwyn, S.D.J. & Hartwick, F.D.A. 1996, *ApJ*, 468, L77
- [10] Fernandez-Soto, A., Lanzetta, K.M., & Yahil, A. 1998, *ApJ*, in press, astro-ph/9809126
- [11] Hogg, D.W. et al. 1998, *AJ*, 115, 1418
- [12] Kodama, T. & Arimoto, N. 1997 *A&A*, 320, 41
- [13] Koo, D.C. 1985, *AJ*, 90, 418
- [14] Lanzetta, K.M., Yahil, A., & Fernandez-Soto, 1996, *Nature*, 381, 759
- [15] Lanzetta, K.M., Yahil, A., & Fernandez-Soto, 1997, astro-ph/9709166
- [16] López-Cruz, O. 1997, Ph. D. Thesis, Univ. of Toronto
- [17] Madau, P. 1995, *ApJ*, 441, 18
- [18] Madau, P., Pozzetti, L., & Dickinson, M.E. 1998, *ApJ*, 498, 106
- [19] Miralles, J.M. & Pelló, R. 1998, astro-ph/980162
- [20] Mobasher, B., Rowan-Robinson, M., Georgakakis, A, & Eaton, N. 1996, *MNRAS*, L7
- [21] Loh, E. & Spillar, E. 1986, *ApJ*, 303, 154
- [22] Williams et al. 1996, *AJ*, 112, 1335
- [23] Steidel, C.C., Giavalisco, M., Dickenson, M., & Adelberger, K.L. 1996, *AJ*, 112, 352
- [24] Sawicki, M.J., Lin, H., & Yee, H.K.C. 1997, *AJ*, 113, 1 (SLY97)
- [25] Sawicki, M.J., & Yee, H.K.C. 1998, *AJ*, 115, 1329
- [26] Sawicki, M.J., Yee, H.K.C., Lin, H. et al. 1999, in preparation
- [27] SubbaRao, M.U., Connolly, A.J., Szalay, A.A, & Koo, D.C. 1996, *AJ*, 112, 929

- [28] Wang, Y., Bahcall, N., & Turner, E.L. 1998, *AJ*, in press, astro-ph/9804195
- [29] Yee, H.K.C., Ellingson, E., & Carlberg, R.G. 1996, *ApJS*, 102, 269
- [30] Yee, H.K.C. et al. 1998, in *IAU General Assembly Joint Discussion on "Redshift Surveys in the 21st Century"*, eds Huchra & Fairall, in press (astro-ph/9710356)
- [31] Yee, H.K.C. et al. 1999, in preparation